

FROM A TO B: NEW METHODS TO INTERPOLATE TWO POSES

HANS-PETER SCHRÖCKER

ABSTRACT. We present two methods to interpolate between two given rigid body displacements. Both are based on linear interpolation in the ambient space of well-known curved point models for the group of rigid body displacements. The resulting motions are either vertical Darboux motions or cubic circular motions. Both are rational of low degree and lie in the cylinder group defined by the two input poses. We unveil the essential parameters in the construction of these motions and discuss some of their properties.

1. INTRODUCTION

Given two poses (position and orientation) of a rigid body in space, there exists a unique helical displacement that maps the first pose to the second. The underlying continuous helical motion can serve as a substitute for a linear interpolant in spatial kinematics and one might believe that there are no natural alternatives to this. However, certain disadvantages of helical interpolants (most notably, helical motions are not algebraic) suggest to look for replacements of linear interpolation.

In this article we present two approaches to the interpolation problem of two poses. They produce low degree rational motions, have a clear geometric background, and come in at least one-parametric families. The underlying algebraic constructions are based on extensions of well-known kinematic mappings from curved manifolds to linear (affine or projective) spaces and might be extended to higher order interpolation. The lack of injectivity of these “extended” kinematic maps may cause problems in certain applications and thus requires a careful investigation of the underlying geometric and algebraic intricacies. Some aspects of this are on the agenda in this article.

In Section 2 we recall two well-known point models, homogeneous transformation matrices and dual quaternions, for the group $SE(3)$ of rigid body displacements and discuss conversion formulas between them. By extending these formulas to the ambient affine or projective space, we construct *extended kinematic mappings* in Section 3. Linear interpolation in the extended dual quaternion model produces vertical Darboux motions whose elementary geometry is well-understood. In Sections 4 and 5 we focus the extended matrix model. We show how to compute the fibers of the corresponding kinematic mapping and we demonstrate the linear interpolation produces cubic circular motions or, more precisely, line symmetric motions with respect to one family of rulings in an orthogonal hyperbolic paraboloid.

2. PRELIMINARIES

We proceed by introducing two well-known point models for the group $SE(3)$ of rigid body displacements and conversion formulas between them. The first model embeds $SE(3)$ into the group of affine maps which can naturally be identified with the affine space \mathbb{R}^{12} . The second model is the projectivised dual quaternion model (Study parameters).

2.1. Point Models for Rigid Body Displacements. With respect to Cartesian coordinate systems in fixed and moving frame, a rigid-body displacement $\varkappa: \mathbb{R}^3 \rightarrow \mathbb{R}^3, x \mapsto y$ can be given in terms of a homogeneous four-by-four transformation matrix:

$$(1) \quad \begin{bmatrix} 1 \\ x \end{bmatrix} \mapsto \begin{bmatrix} 1 \\ y \end{bmatrix} = \begin{bmatrix} 1 & 0^T \\ a & A \end{bmatrix} \cdot \begin{bmatrix} 1 \\ x \end{bmatrix}.$$

Here, A is an orthogonal matrix of dimension 3×3 and determinant 1. If A fails to satisfy the orthogonality conditions, (1) describes an affine map. In this sense, the space of affine maps — which may be identified with $\mathbb{R}^{12} \cong (A, a)$ — provides a point model for the group $SE(3)$ of rigid-body displacements. In this space, $SE(3)$ is the algebraic variety defined by the six quadratic equations resulting from $A \cdot A^T = I_3$ (the identity matrix of dimension 3×3) and the cubic equation $\det A = 1$. This variety is of dimension and co-dimension six and its ideal contains no linear equations.

Another important point model of $SE(3)$ is *Study parameters*. These are most conveniently described in terms of dual quaternions which we briefly introduce. For more details we refer to [1, 4, 5]. A quaternion p is an element of the four-dimensional real associative algebra \mathbb{H} , generated by the base elements $1, \mathbf{i}, \mathbf{j}, \mathbf{k}$ and the multiplication rules

$$\mathbf{i}^2 = \mathbf{j}^2 = \mathbf{k}^2 = \mathbf{ijk} = -1.$$

It may be written as $p = p_0 + p_1\mathbf{i} + p_2\mathbf{j} + p_3\mathbf{k}$ with $p_0, p_1, p_2, p_3 \in \mathbb{R}$. The *conjugate quaternion* is defined

Date: June 15, 2017.

2010 Mathematics Subject Classification. Primary 70B10; Secondary 65D17, 14R25.

as $\bar{p} := p_0 - p_1\mathbf{i} - p_2\mathbf{j} - p_3\mathbf{k}$, the *quaternion norm* $p\bar{p} = p_0^2 + p_1^2 + p_2^2 + p_3^2$ is a non-negative real number.

The algebra \mathbb{DH} of dual quaternions is obtained by extension of scalars from the real numbers \mathbb{R} to the dual numbers $\mathbb{D} = \mathbb{R}[\varepsilon]/\langle\varepsilon^2\rangle$. Any dual number may be written as $r = s + \varepsilon t$ with $s, t \in \mathbb{R}$. Multiplication obeys the rule $\varepsilon^2 = 0$ so that $(s + \varepsilon t)(u + \varepsilon v) = su + \varepsilon(sv + tu)$. Any dual quaternion h can be written as $h = p + \varepsilon q$ with quaternions p (the primal part) and q (the dual part). Defining also the dual quaternion conjugate $\bar{h} := \bar{p} + \varepsilon\bar{q}$, the dual quaternion norm is $h\bar{h} = p\bar{p} + \varepsilon(p\bar{q} + q\bar{p})$. It is a dual number whose dual part (the coefficient of ε) vanishes precisely if the Study condition

$$(2) \quad p\bar{q} + q\bar{p} = 0$$

is satisfied. Dual quaternions are related to spatial kinematics by an isomorphism from $\text{SE}(3)$ to a certain subgroup constructed from \mathbb{DH} . We embed \mathbb{R}^3 into \mathbb{H} via $(x_1, x_2, x_3) \in \mathbb{R}^3 \mapsto x = x_1\mathbf{i} + x_2\mathbf{j} + x_3\mathbf{k}$ and define the action of $h = p + \varepsilon q$ with norm $h\bar{h} \in \mathbb{R} \setminus \{0\}$ on x by

$$(3) \quad 1 + \varepsilon x \mapsto (p\bar{p})^{-1}(p - \varepsilon q) \cdot (1 + \varepsilon x) \cdot (\bar{p} + \varepsilon\bar{q}).$$

The map (3) is a rigid body displacement. With $p = p_0 + p_1\mathbf{i} + p_2\mathbf{j} + p_3\mathbf{k}$ and $q = q_0 + q_1\mathbf{i} + q_2\mathbf{j} + q_3\mathbf{k}$, the entries of the homogeneous vector $[p_0, p_1, p_2, p_3, q_0, q_1, q_2, q_3]$ are called the *Study parameters* of the displacement (3). The composition of displacements in Study parameters is just the dual quaternion multiplication. Thus, $\text{SE}(3)$ is isomorphic to the group of dual quaternions of unit norm, modulo the multiplicative real group. Study parameters allow for a bilinear composition of displacements with a minimal number of parameters but have other advantages as well.

Since the Study parameters are only determined up to multiplication with a non-zero real scalar, the underlying point model of $\text{SE}(3)$ is contained in real projective space P^7 of dimension seven. More precisely, the bilinear form $p + \varepsilon q \mapsto p\bar{q} + q\bar{p}$ (compare with Equation (2)) defines a quadric $\mathcal{S} \subset P^7$, the so-called *Study quadric*. Rigid body displacements are in bijection to points of \mathcal{S} minus the *exceptional generator* E , given by the equation $p = 0$.

2.2. Conversion Formulas. Formulas for the conversion between homogeneous transformation matrices and Study parameters are well-known. A straightforward calculation shows that the displacement given by $h = p + \varepsilon q$ via (3) is also given by the matrix

$$(4) \quad A = \frac{1}{\Delta} \begin{bmatrix} \Delta & 0 & 0 & 0 \\ a_1 & a_{11} & a_{12} & a_{13} \\ a_2 & a_{21} & a_{22} & a_{23} \\ a_3 & a_{31} & a_{32} & a_{33} \end{bmatrix}$$

where $\Delta = p_0^2 + p_1^2 + p_2^2 + p_3^2$,

$$\begin{aligned} a_{11} &= p_0^2 + p_1^2 - p_2^2 - p_3^2, & a_{12} &= 2(p_1p_2 - p_0p_3), \\ a_{13} &= 2(p_0p_2 + p_1p_3), & a_{21} &= 2(p_0p_3 + p_1p_2), \\ a_{22} &= p_0^2 - p_1^2 + p_2^2 - p_3^2, & a_{23} &= 2(p_2p_3 - p_0p_1), \\ a_{31} &= 2(p_1p_3 - p_0p_2), & a_{23} &= 2(p_0p_1 + p_2p_3), \\ a_{33} &= p_0^2 - p_1^2 - p_2^2 + p_3^2, \end{aligned}$$

and

$$(5) \quad \begin{aligned} a_1 &= 2(-p_0q_1 + p_1q_0 - p_2q_3 + p_3q_2), \\ a_2 &= 2(-p_0q_2 + p_1q_3 + p_2q_0 - p_3q_1), \\ a_3 &= 2(-p_0q_3 - p_1q_2 + p_2q_1 + p_3q_0). \end{aligned}$$

In order to invert this calculation, we have to find a dual quaternion $h = p + \varepsilon q$ that satisfies the Study condition and describes the displacement (1) with orthogonal matrix $A = (a_{ij})_{i,j=1,\dots,3}$ and vector $a = (a_1, a_2, a_3)^\top$. To begin with, the dual part q can be computed from primal part p and a : Augmenting (5) with the Study condition $p_0q_0 + p_1q_1 + p_2q_2 + p_3q_3 = 0$ gives a system of linear equations for q_0, q_1, q_2 , and q_3 with determinant $\Delta^2 \neq 0$. Provided p is normalised, its unique solution is

$$(6) \quad \begin{bmatrix} q_0 \\ q_1 \\ q_2 \\ q_3 \end{bmatrix} = \frac{1}{2} \begin{bmatrix} 0 & a_1 & a_2 & a_3 \\ -a_1 & 0 & a_3 & -a_2 \\ -a_2 & -a_3 & 0 & a_1 \\ -a_3 & a_2 & -a_1 & 0 \end{bmatrix} \cdot \begin{bmatrix} p_0 \\ p_1 \\ p_2 \\ p_3 \end{bmatrix}.$$

Hence, we may focus on the primal part. Comparing coefficients of A with (4) we find

$$(7) \quad \begin{aligned} p_0^2 &= \frac{1}{4}(1 + a_{11} + a_{22} + a_{33}), \\ p_1^2 &= \frac{1}{4}(1 + a_{11} - a_{22} - a_{33}), \\ p_2^2 &= \frac{1}{4}(1 - a_{11} + a_{22} - a_{33}), \\ p_3^2 &= \frac{1}{4}(1 - a_{11} - a_{22} + a_{33}) \end{aligned}$$

so that all coefficients of p are determined up to sign. Moreover, we have

$$(8) \quad \begin{aligned} p_0p_1 &= \frac{1}{4}(a_{32} - a_{23}), & p_0p_2 &= \frac{1}{4}(a_{13} - a_{31}), \\ p_0p_3 &= \frac{1}{4}(a_{21} - a_{12}), & p_1p_2 &= \frac{1}{4}(a_{21} + a_{12}), \\ p_1p_3 &= \frac{1}{4}(a_{31} + a_{13}), & p_2p_3 &= \frac{1}{4}(a_{32} + a_{23}). \end{aligned}$$

From (7) and (8) we see that the ratio of the primal part coefficients (the so-called *Euler parameters*) is given as

$$(9) \quad \begin{aligned} p_0 : p_1 : p_2 : p_3 &= \\ 1 + a_{11} + a_{22} + a_{33} : a_{32} - a_{23} : a_{13} - a_{31} : a_{21} - a_{12} &= \\ a_{32} - a_{23} : 1 + a_{11} - a_{22} - a_{33} : a_{21} + a_{12} : a_{31} + a_{13} &= \\ a_{13} - a_{31} : a_{21} + a_{12} : 1 - a_{11} + a_{22} - a_{33} : a_{32} + a_{23} &= \\ a_{21} - a_{12} : a_{31} + a_{13} : a_{32} + a_{23} : 1 - a_{11} - a_{22} + a_{33}. \end{aligned}$$

Any of the four ratios may be used to compute p up to irrelevant scalar multiples unless it gives $0 : 0 : 0 : 0$. This is the case for half-turns ($p_0 = 0$) or rotations around vectors

parallel to a coordinate plane ($p_1 = 0$, $p_2 = 0$, or $p_3 = 0$). At least one of the four ratios in (9) is always valid.

For a geometric study of these relations, we take a more general point of view. We embed the space of three by three matrices into \mathbb{R}^9 by the inclusion map

$$\begin{aligned} A &\hookrightarrow (x_1, x_2, x_3, x_4, x_5, x_6, x_7, x_8, x_9)^\top \\ &= (a_{11}, a_{12}, a_{13}, a_{21}, a_{22}, a_{23}, a_{31}, a_{32}, a_{33})^\top. \end{aligned}$$

For $\ell \in \{0, 1, 2, 3\}$, we define a linear map $\mu'_\ell: \mathbb{R}^{10} \rightarrow \mathbb{R}^4$ via

$$\begin{aligned} (10) \quad \mu'_0(x) &:= (x_0 + x_1 + x_5 + x_9, x_8 - x_6, x_3 - x_7, x_4 - x_2) \\ \mu'_1(x) &:= (x_8 - x_6, x_0 + x_1 - x_5 - x_9, x_4 + x_2, x_7 + x_3), \\ \mu'_2(x) &:= (x_3 - x_7, x_4 + x_2, x_0 - x_1 + x_5 - x_9, x_8 + x_6), \\ \mu'_3(x) &:= (x_4 - x_2, x_7 + x_3, x_8 + x_6, x_0 - x_1 - x_5 + x_9). \end{aligned}$$

These maps are constructed such that the dehomogenisation $x_0 = 1$ produces a vector $\mu'_\ell(x)$ that after normalisation yields the coefficients of the ℓ -th proportion in (9). This anticipates the projective viewpoint we will adopt a little later. Even more generally, we define a family

$$(11) \quad \begin{aligned} \mu'_m: \mathbb{R}^{10} &\rightarrow \mathbb{R}^4, \\ x &\mapsto m_0 \mu'_0(x) + m_1 \mu'_1(x) + m_2 \mu'_2(x) + m_3 \mu'_3(x) \end{aligned}$$

of maps which is parameterised by the vector $m = (m_0, m_1, m_2, m_3)^\top \in \mathbb{R}^4$. The map μ'_m can be extended to a family of maps

$$(12) \quad \begin{aligned} \mu_m: \mathbb{R}^{13} &\rightarrow \mathbb{R}^8, \\ (x, a_1, a_2, a_3)^\top &\mapsto (p_0, p_1, p_2, p_3, q_0, q_1, q_2, q_3)^\top \end{aligned}$$

where $(p_0, p_1, p_2, p_3)^\top = \mu'_m(x)$ and $(q_0, q_1, q_2, q_3)^\top$ is computed via (6). Any map μ_m takes a rigid body displacement given as homogeneous matrix to a vector of Study parameters, unless the image is the zero vector.

3. EXTENDED KINEMATIC MAPPINGS

So far, we introduced two point models for $\text{SE}(3)$ and explained conversion formulas between both models. The first model is a certain variety in the space \mathbb{R}^{12} of affine maps, defined by orthogonality of the linear component and positivity of its determinant. The second model is the Study quadric $\mathcal{S} \subset P^7$ minus the exceptional generator E .

At the core of this article stands the observation that the conversion formulas between both point models can formally be extended to the complete ambient space \mathbb{R}^{12} or P^7 , respectively, and still yield a well-defined rigid body displacement in the other model. This gives rise to *extended kinematic mappings* or, considering (12), even a family of such extended mappings.

One of the biggest advantages of these mappings is that they eliminate the non-linearity of the underlying point space. This comes, however, at the cost of losing injectivity

whence one is led to study the induced fibers (pre-images of single displacements.) Other interesting questions pertain to kinematic interpretations of “simple” curves. In particular, we may ask for the motion corresponding to a straight line connecting two given poses. We will provide a detailed answer to these questions for the extended kinematic mappings (12). Before doing this, we consider the extended kinematic mapping from $\varkappa: P^7 \setminus E \rightarrow \text{SE}(3)$ that is defined by Equations (4) and (5). Since it has already been studied elsewhere [1, 8, 9], we confine ourselves to briefly stating some facts of interest but omit proofs:

- The fiber of the displacement represented by the dual quaternion $h = p + \varepsilon q$ is the straight line spanned by h and εq [8].
- The \varkappa -image of a motion connecting two poses by a straight line segment is a vertical Darboux motion [1, 9].

Recall that a *vertical Darboux motion* is the composition of a rotation around a fixed axis with a translation in direction of this axis where rotation angle φ and translation distance z are coupled by a sine function ($z = \lambda \sin(\varphi + \varkappa)$; $\lambda, \varkappa \in \mathbb{R}$) [1, Chapter 9, §7]. Special cases include $\lambda = 0$ (rotation) and the limit for $\lambda \rightarrow \infty$ (translation).

The vertical Darboux motion has quite a few interesting properties which we state below in form of a theorem. (Not because they are new but because we want to emphasise similarities to the motion obtained as μ_m -image of a straight line in Theorem 2). Before doing so, we introduce a few more concepts. A motion group generated by rotations around and translations parallel to a fixed axis is called a *cylinder group*. An element of a cylinder group is fully specified by rotation angle φ and signed translation distance z , both measured with respect to a fixed initial position. A motion in a cylinder group is fully specified, if φ and z are functions of a common parameter t . We call the thus described parametric curve in the $[\varphi, z]$ -plane the motion’s *transmission curve*. Finally, a line-symmetric motion is the motion obtained by rotating the moving space about the generators of a ruled surface through 180° .

Theorem 1. *The vertical Darboux motion has the following properties:*

1. *It is a motion in a cylinder group (Figure 1).*
2. *It is line-symmetric with respect to the rulings of a Plücker conoid [6] (Figure 2).*
3. *The transmission curve of a vertical Darboux motion is a scaled and shifted sine curve (Figure 1).*
4. *The trajectories of points are rational curves of degree two (ellipses or, in special cases, straight line segments; Figure 1).*

Given a start and an end pose, there exists a two-parametric set of lines connecting a point in the fiber of the start pose with a point in the fiber of the end pose. These correspond to certain variations of λ and \varkappa . Considering

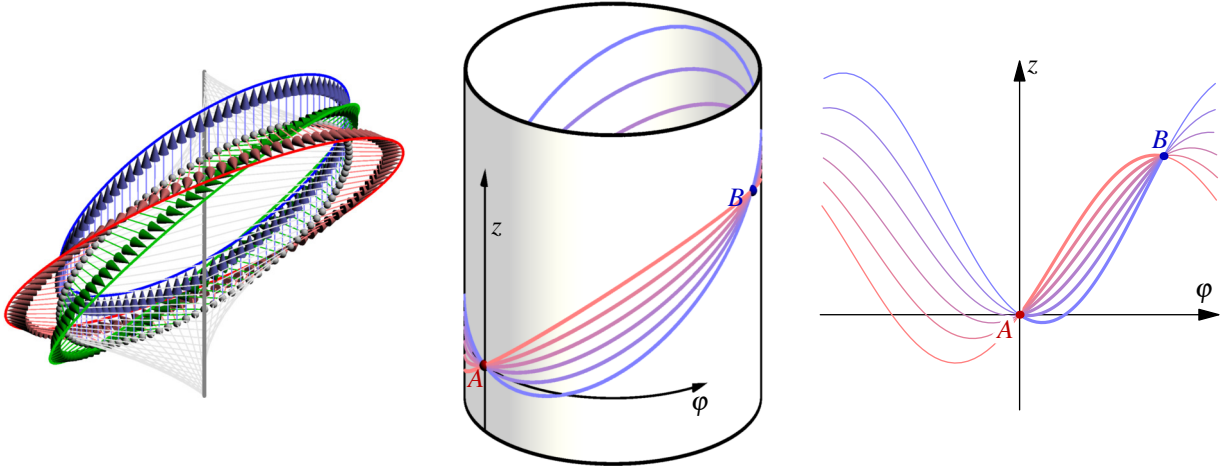


FIGURE 1. Vertical Darboux motion (left), trajectories connecting A and B (centre) and relationship between rotation angle ϕ and translation distance z (right).

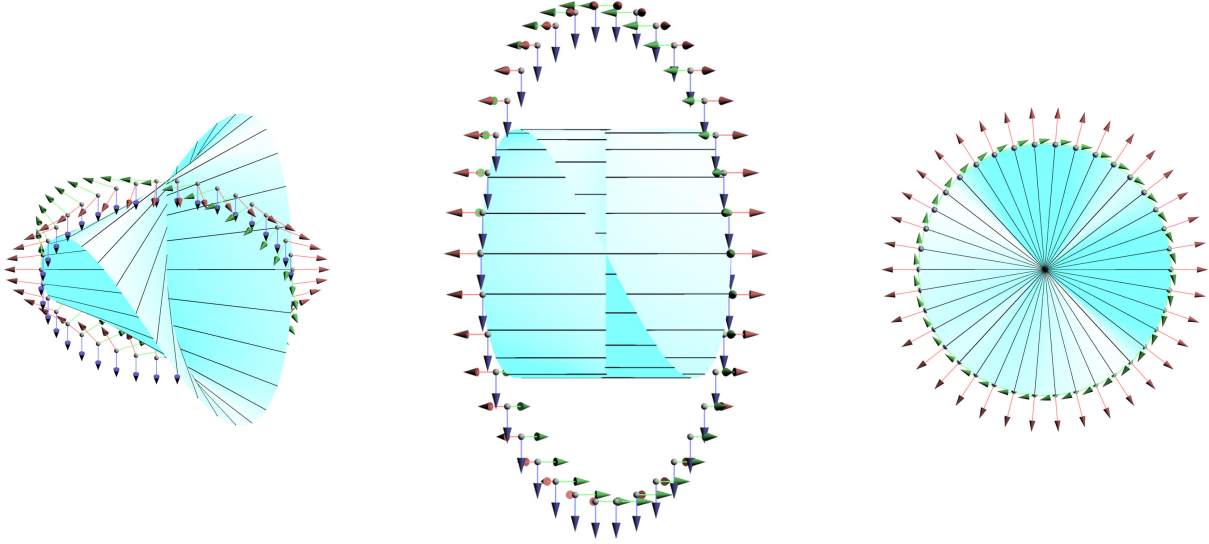


FIGURE 2. Line-symmetric motion with respect to a Plücker conoid

these changes modulo the fibration, only one essential parameter remains. This can also be explained by Number 3 in Theorem 1. Other statements on the interpolant are:

- There exists exactly one Darboux motion that interpolates the two given poses and contains a third pose in their cylinder group.
- It is possible to prescribe the instantaneous pitch (ratio of angular velocity and translational velocity) in start or end point but not in both.
- There is a distinguished interpolant where start and end point on the transmission curve are at the same distance to an inflection point.

In the following sections, we aim at comparable statements for the extended kinematic map μ_m . Indeed, we will

see many similarities between the motions resulting from both maps.

4. BASIC PROPERTIES AND FIBERS

The aim of this section is a more detailed study of the basic geometry of the maps μ_m and μ'_m . An important observation is that μ'_m , as defined in (11) induces a *projective map* whose restriction to the affine sheet $x_0 = 1$ translates between orthogonal matrices and quaternions. We denote this projective map by $\mu'_{[m]}$ since it only depends on the *point* $[m] \in P^3$ and not the *vector* $m \in \mathbb{R}^4$. Its matrix representation reads $[x_0, \dots, x_9]^T \mapsto M_m \cdot [x_0, \dots, x_9]^T$ where

$M_m = [M_1, M_2]$ and

$$M_1 = \begin{bmatrix} m_0 & m_0 & -m_3 & m_2 & m_3 \\ m_1 & m_1 & m_2 & m_3 & m_2 \\ m_2 & -m_2 & m_1 & m_0 & m_1 \\ m_3 & -m_3 & -m_0 & m_1 & m_0 \end{bmatrix},$$

$$M_2 = \begin{bmatrix} m_0 & -m_1 & -m_2 & m_1 & m_0 \\ -m_1 & -m_0 & m_3 & m_0 & -m_1 \\ m_2 & m_3 & -m_0 & m_3 & -m_2 \\ -m_3 & m_2 & m_1 & m_2 & m_3 \end{bmatrix}.$$

The map $\mu'_{[m]}$ is not defined on the projective space N_m over the nullspace of M_m . This space is spanned by the vectors

$$(13) \quad \begin{aligned} f_0 &:= (n_1n_2, -n_2n_4, n_0, 0, 0, -n_1n_5, 0, 0, 0, n_4n_5)^\top, \\ f_1 &:= (-n_4n_6, n_1n_6, 0, n_0, 0, -n_1n_3, 0, 0, 0, n_3n_4)^\top, \\ f_2 &:= (-n_4n_5, n_1n_5, 0, 0, n_0, n_2n_4, 0, 0, 0, -n_1n_2)^\top, \\ f_3 &:= (n_2n_3, n_5n_6, 0, 0, 0, -n_3n_5, n_0, 0, 0, -n_2n_6)^\top, \\ f_4 &:= (n_1n_3, -n_3n_4, 0, 0, 0, n_4n_6, 0, n_0, 0, -n_1n_6)^\top, \\ f_5 &:= (-n_5n_6, -n_2n_3, 0, 0, 0, n_2n_6, 0, 0, n_0, n_3n_5)^\top. \end{aligned}$$

where

$$(14) \quad \begin{aligned} n_0 &:= 4m_0m_1m_2m_3, \quad n_1 := m_0m_1 - m_2m_3, \\ n_2 &:= m_0m_2 - m_1m_3, \quad n_3 := m_0m_3 - m_1m_2, \\ n_4 &:= m_0m_1 + m_2m_3, \quad n_5 := m_0m_2 + m_1m_3, \\ n_6 &:= m_0m_3 + m_1m_2. \end{aligned}$$

The dimension of N_m is six unless $m = 0$ whence M_m is the zero matrix and the map $\mu_{[m]}$ becomes undefined. The basis vectors in (13) correspond to the matrices that we denote by F_0, \dots, F_5 , respectively.

The family of maps (12) induces a family of maps from P^{12} to P^7 which we similarly denote by $\mu_{[m]}$. The first four coordinate functions are linear, the last four are quadratic. Moreover, the maps are linear in a_0, a_1, a_2 , and a_3 . Thus, the $\mu_{[m]}$ -image of all displacements with fixed orientation is a projective subspace of dimension four, — a left co-set of the translation group. The base set of $\mu'_{[m]}$ is the projective space $[N_m]$ over the nullspace of $\mu'_{[m]}$. The $\mu'_{[m]}$ -fiber $\mathcal{F}'_{[m]}([x'])$ of a point $[x'] \in P^9$ (the preimage of $\mu'_{[m]}([x'])$) is the projective subspace $[x'] \vee [N_m]$.

In order to describe the $\mu_{[m]}$ -fiber $\mathcal{F}_{[m]}([x])$ of $[x] \in P^{12}$, we introduce some more notation. Given $x = (x_0, \dots, x_{12}) \in \mathbb{R}^{13}$, we denote its projection on the rotational component by $x' := (x_0, \dots, x_9, 0, 0, 0)$ and its projection on the translational component by $x'' := (0, \dots, 0, x_{10}, x_{11}, x_{12})$. The $\mu_{[m]}$ -fiber of $[x] \in P^{12}$ is then

$$(15) \quad \mathcal{F}_{[m]}([x]) = x_0 \mathcal{F}'_{[m]}([x']) + \psi [x'']$$

where ψ is the homogenising coordinate (entry in the top left corner) of $\mathcal{F}'_{[m]}$.

5. IMAGE OF STRAIGHT LINES

Now we come to a central part of this article. We consider two poses A_0, B_0 and linear interpolants in \mathbb{R}^{12} constructed from them. Without loss of generality, we assume that A_0 is the identity and

$$B_0 = \begin{bmatrix} 1 & 0 & 0 & 0 \\ 0 & \cos \varphi & -\sin \varphi & 0 \\ 0 & \sin \varphi & \cos \varphi & 0 \\ d & 0 & 0 & 1 \end{bmatrix}$$

with fixed values $\varphi \in [0, 2\pi)$ and $d \in \mathbb{R}$. It is not sufficient to just consider the straight line connecting A_0 and B_0 but we should study the lines in the set

$$\{A \vee B \mid A \in \mathcal{F}_{[m]}(A_0), B \in \mathcal{F}_{[m]}(B_0)\}.$$

The elements $A' \in \mathcal{F}'_{[m]}(A'_0)$ and $B' \in \mathcal{F}'_{[m]}(B'_0)$ can be written as

$$A' = A'_0 + \sum_{\ell=0}^5 \alpha_\ell F_\ell, \quad B' = B'_0 + \sum_{\ell=0}^5 \beta_\ell F_\ell$$

where $(\alpha_0, \dots, \alpha_5)^\top, (\beta_0, \dots, \beta_5)^\top \in \mathbb{R}^6$. The elements of $\mathcal{F}_{[m]}(A_0)$ and $\mathcal{F}_{[m]}(B_0)$ can then be computed by (15) with obvious adaptations to matrix notation. The span of A and B can be parameterized as $C = t_0A + t_1B$ with $[t_0, t_1]^\top \in P^1$ or, using an inhomogeneous parameter t with $(1-t) : t = t_0 : t_1$, as $C = (1-t)A + tB$. Then $c := \mu_{[m]}(C)$ is a polynomial of degree two over the ring $\mathbb{D}\mathbb{H}$. Motions of this type are the topic of [3]. They are *line-symmetric* with respect to a regulus, that is, they can be generated by reflecting a fixed frame of reference in one family of rulings of a *quadric* \mathcal{Q} . A more detailed look at the coordinate functions of c will reveal that our case is even more special. We have $c(t) = [c_0, 0, 0, c_3, c_4, 0, 0, c_7]^\top$ where

$$(16) \quad \begin{aligned} c_0 &= -g_1((m_0(\cos \varphi - 1) + m_3 \sin \varphi)t + 2m_0), \\ c_3 &= g_1(m_3(\cos \varphi - 1) - m_0 \sin \varphi)t, \\ c_4 &= -g_1^{-1}g_2c_3, \quad c_7 = g_1^{-1}g_2c_0. \end{aligned}$$

Here, we abbreviate $g_1 = -2((1-t)a + tb + 1)$ and $g_2 = td(b+1)$ where

$$\begin{aligned} a &:= n_1n_2\alpha_0 - n_4n_6\alpha_1 - \\ &\quad n_4n_5\alpha_2 + n_2n_3\alpha_3 + n_1n_3\alpha_4 - n_5n_6\alpha_5, \\ b &:= n_1n_2\beta_0 - n_4n_6\beta_1 - \\ &\quad n_4n_5\beta_2 + n_2n_3\beta_3 + n_1n_3\beta_4 - n_5n_6\beta_5 \end{aligned}$$

and the values of n_1, \dots, n_6 are given in (14). We thus have:

1. The motion parameterised by c lies in the cylinder group generated by the rotations about and translations in the third coordinate direction. More generally, any motion corresponding to a line in \mathbb{R}^{12} lies in a cylinder group.
2. The degree of c in t is two but the primal part has the common real polynomial factor g_1 of degree one. For

the zero of g_1 , the primal part vanishes and the corresponding motion becomes undefined. This is equivalent with the quadric \mathcal{Q} being a *hyperbolic paraboloid* [3]. The corresponding motion is called a *cubic circular motion* [1] (Figure 3).

3. The parametric equation of c formally depends on numerous parameters that are independent from the displacements A and B : The homogeneous vector $[m_0, m_1, m_2, m_3]^\top$ determines the map $\mu_{[m]}$; $\alpha_0, \dots, \alpha_5$ determine the point in $\mathcal{F}(A_0)$ and β_0, \dots, β_5 determine the point in $\mathcal{F}(B_0)$. However, only m_0, m_3, a and b occur in (16).

The fact that the motion c lies in a cylinder group suggests to compute rotation angle ω and translation distance z . This will help us to assess more precisely the meaning of the parameters m_0, m_3, a and b . From (17)

$$\tan \frac{\omega}{2} = \frac{c_3}{c_0} = -\frac{(m_3(\cos \varphi - 1) - m_0 \sin \varphi)t}{(m_0(\cos \varphi - 1) + m_3 \sin \varphi)t + 2m_0}$$

we see that the rotation angle depends only on m_0 and m_3 (and φ). From

$$(18) \quad z = -\frac{2g_2}{g_1} = \frac{td(b+1)}{(1-t)a+tb+1}$$

we see that z depends only on a and b (and d). The functional relationship between translation distance z and rotation angle ω for varying parameters is displayed in Figure 3, right.

Moreover, we infer from (17) and (18) that $\tan \frac{\omega}{2}$ and z fulfill a functional relation of the shape

$$(pt + q) \tan \frac{\omega}{2} = (rt + s)z$$

where p, q, r , and s are real numbers depending on m_0, m_3, a, b, d , and φ that can easily be computed. This demonstrates that the curves depicted in Figure 3 are *translated and scaled (in ω - and z -direction) copies of the graph of the tangent function*. Consequences of this observation are, for example:

- There is a two-parametric family of cubic circular motions interpolating two prescribed poses.
- For any given interpolant, the respective slopes at start- and endpoint of any trajectory with respect to the z -axis have the same sign.

We already know that any motion corresponding to a straight line in \mathbb{R}^{12} by virtue of the kinematic map $\mu_{[m]}$ is line symmetric with respect to one regulus on a hyperbolic paraboloid. Moreover, it is contained in a cylinder group. Now we show that the latter property is equivalent to the orthogonality of the underlying hyperbolic paraboloid.

Consider the hyperbolic paraboloid Φ given by the quadratic form

$$[x_0, x_1, x_2, x_3]^\top \mapsto x_0x_3 + \frac{x_1^2}{a^2} - \frac{x_2^2}{b^2}$$

with $a, b \in \mathbb{R} \setminus \{0\}$. One set of rulings of this surface admits the parametric equation

$$[4at^2, 4bt^2, 4t, b, a, -2abt]^\top, \quad t \in \mathbb{R} \cup \{\infty\}$$

in Plücker line coordinates. Its line-symmetric motion in the dual quaternion model is obtained as

$$c(t) = 4t((a\mathbf{i} + b\mathbf{j})t + \mathbf{k}) + \varepsilon(2ab\mathbf{k}t - b\mathbf{i} - a\mathbf{j}).$$

Our aim is to find a necessary and sufficient condition for this motion to lie in a cylinder group. To this end, we write $c(t) = 4(a\mathbf{i} + b\mathbf{j})F_1F_2$ where

$$F_1 = t - \frac{1}{a^2 + b^2}(b\mathbf{i} - a\mathbf{j}) + \varepsilon \frac{a^2 - b^2}{4(a^2 + b^2)}(a\mathbf{i} + b\mathbf{j})$$

and

$$F_2 = t - \frac{1}{4}\varepsilon(a\mathbf{i} - b\mathbf{j}).$$

(Since t serves as a real motion parameter, it is natural to define multiplication of polynomials over the non-commutative ring $\mathbb{D}\mathbb{H}$ by the *convention* that the indeterminate t commutes with the dual quaternion coefficients.) This shows that the motion is a composition of a translational motion in direction of the vector $(a, -b, 0)^\top$, given by the last factor F_2 , a rotation about an axis parallel to $(b, -a, 0)^\top$, given by the middle factor F_1 , and a constant rotation, given by the first factor. Translation direction and rotation axis are parallel if and only if $a = \pm b$ and this is equivalent with the orthogonality of the underlying hyperbolic paraboloid. The corresponding line symmetric motion is not unheard of in German literature [1, 2, 7]. It is visualised in Figures 3 and 4.

We summarise our findings of this section in

Theorem 2. *The motion obtained as μ -image of a straight line has the following properties:*

1. *It is a motion in a cylinder group.*
2. *It is line-symmetric with respect to one family of rulings on an orthogonal hyperbolic paraboloid. [6] (Figure 4).*
3. *The transmission curve is a scaled and shifted tangent curve (Figure 3, right).*
4. *The trajectories of points are rational curves of degree three with exactly one point at infinity; the curve's orthographic projection in direction of this point is a circle (Figure 4, right).*

The last statement follows easily from either the geometric generation or the parametric representation $c(t)$ of the motion.

6. SUMMARY AND OUTLOOK

We have presented two methods to interpolate between two given poses A and B by linear interpolation in a point model of $\text{SE}(3)$, extended to the ambient projective or affine space. The resulting motions are vertical Darboux motions in one and cubic circular motions in the other case.

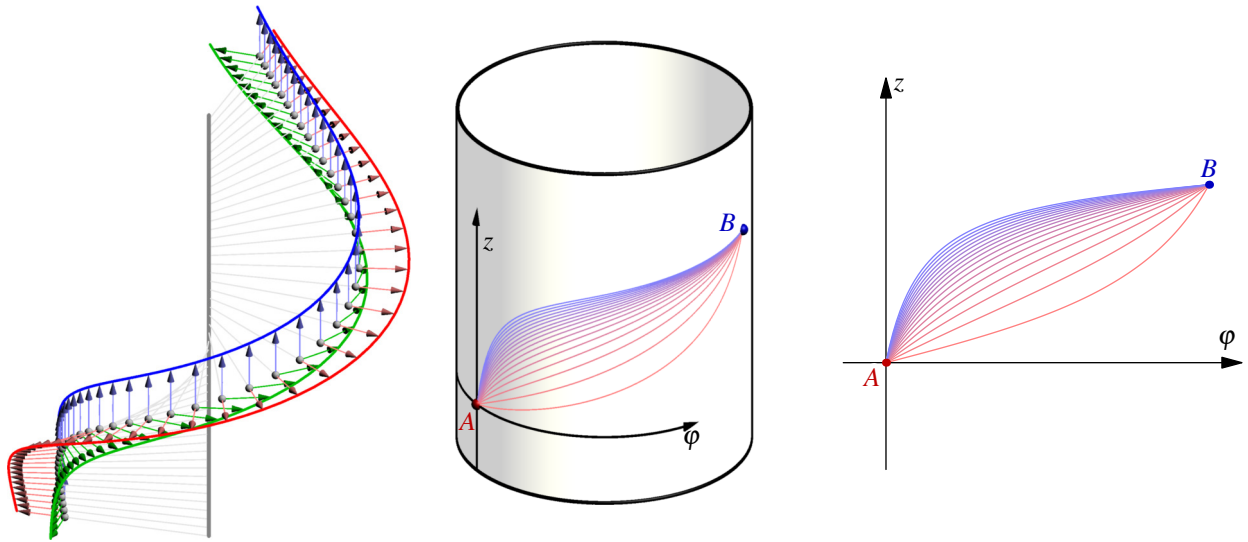


FIGURE 3. Circular cubic motion (left), trajectories connecting A and B (centre) and relationship between rotation angle φ and translation distance z (right).

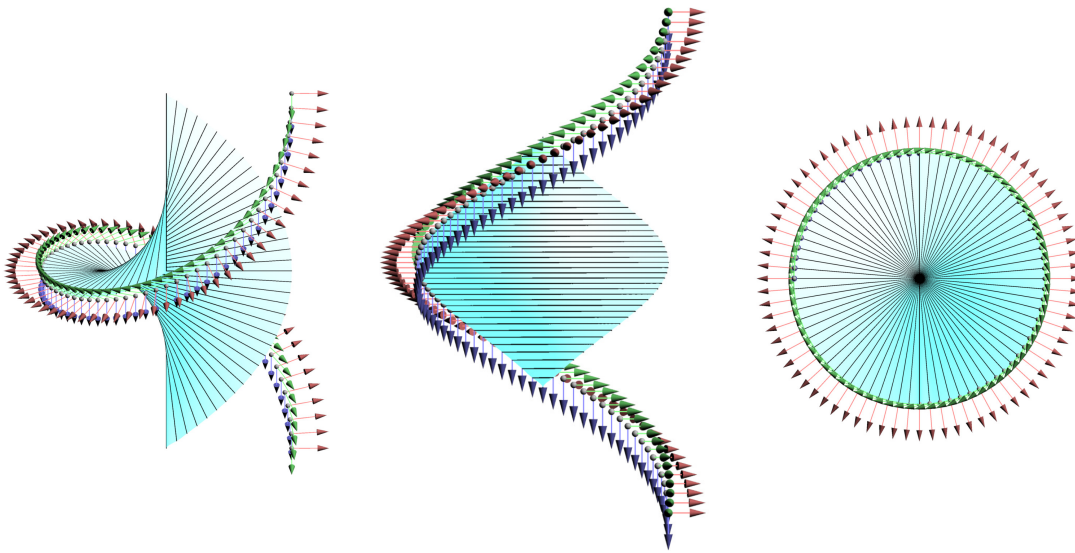


FIGURE 4. Line-symmetric motion with respect to an orthogonal hyperbolic paraboloid

More precisely, the latter motions turned out to be line symmetric with respect to an orthogonal hyperboloid.

An interesting feature of the extended matrix point model of $SE(3)$ is that it automatically comes with an affine structure. This allows to directly employ affine constructions of Computer Aided Design, like the algorithms of de Casteljau and de Boor or certain subdivision schemes, to motions — something that is not always possible with other curved models of $SE(3)$. Via the map $\mu_{[m]}$ the CAD constructions propagate to $SE(3)$. The map $\mu_{[m]}$ is not invertible which may result in unwanted behaviour with respect to motion singularities or numerics. Nonetheless, it

seems to be a promising and straightforward idea for adapting CAD curve design techniques to motion design which deserves further attention. A proof of concept is presented in Figure 6 where a cubic Bézier curve in \mathbb{R}^{12} is mapped, via $\mu_{[m]}$, to a planar motion. The “control poses” are rigid body displacements and not affinely distorted. The “sides” of the control polygon are planar versions of cubic circular motions, that is, rotations.

ACKNOWLEDGEMENTS

This work was supported by the Austrian Science Fund (FWF): P 26607 (Algebraic Methods in Kinematics: Motion Factorisation and Bond Theory).

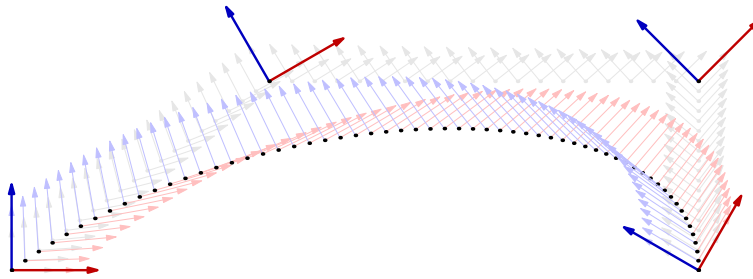


FIGURE 5. A cubic Bézier motion via de Casteljau's algorithm and the extended kinematic map $\mu_{[m]}$

REFERENCES

- [1] O. Bottema and B. Roth, *Theoretical kinematics*, Dover Publications, 1990.
- [2] Anton Grünwald, *Die kubische Kreisbewegung eines starren Körpers*, *Z. Math. Physik* **55** (1907), 264–296.
- [3] Marco Hamann, *Line-symmetric motions with respect to reguli*, *Mech. Machine Theory* **46** (2011), no. 7, 960–974.
- [4] Manfred Husty and Hans-Peter Schröcker, *Kinematics and algebraic geometry*, 21st century kinematics. the 2012 nsf workshop, 2012, pp. 85–123.
- [5] Daniel Klawitter, *Clifford algebras. geometric modelling and chain geometries with application in kinematics*, Springer Spektrum, 2015.
- [6] J. Krames, *Zur aufrechten Ellipsenbewegung des Raumes (Über symmetrische Schrotungen III)*, *Monatsh. Math. Physik* **46** (1937), no. 1, 38–50.
- [7] J. Krames, *Zur Geometrie des Bennett'schen Mechanismus (Über symmetrische Schrotungen IV)*, Österreich. Akad. Wiss. Math.-Natur. Kl. S.-B. II **146** (1937), 159–173.
- [8] Martin Pfurner, Hans-Peter Schröcker, and Manfred Husty, *Path planning in kinematic image space without the Study condition*, Proceedings of advances in robot kinematics, 2016.
- [9] Anurag Purwar and Jeff Ge, *Kinematic convexity of rigid body displacements*, Proceedings of the asme 2010 international design engineering technical conferences & computers and information in engineering conference idetc/cie, 2010.
- [10] Tudor-Dan Rad, Daniel F. Scharler, and Hans-Peter Schröcker, *The kinematic image of RR, PR, and RP dyads*, 2016.
- [11] B. Ravani and B. Roth, *Mappings of spatial kinematics*, *J. Mech., Trans., and Automation* **106** (1984), no. 3, 341–347.
- [12] Jon Selig, *Geometric fundamentals of robotics*, 2nd ed., Monographs in Computer Science, Springer, 2005.
- [13] Walter Wunderlich, *Kubische Zwangläufe*, Österreich. Akad. Wiss. Math.-Natur. Kl. S.-B. II **193** (1984), 45–68.

(Hans-Peter Schröcker) UNIT GEOMETRY AND CAD, UNIVERSITY OF INNSBRUCK, TECHNIKERSTR. 13, 6020 INNSBRUCK, AUSTRIA

URL: <http://geometrie.uibk.ac.at/schroecker/>

E-mail address: hans-peter.schroecker@uibk.ac.at